PCS-T2R-050

LARGE-SCALE TEST DATA EVALUATION

May 1995

R. P. Ofstun
D. Spencer

WESTINGHOUSE ELECTRIC CORPORATION
ENERGY SYSTEMS BUSINESS UNIT
ADVANCED TECHNOLOGY BUSINESS AREA
P.O. BOX 355
PITTSBURGH, PENNSYLVANIA 15230

TABLE OF CONTENTS

SUMMARY

The large-scale test facility[1,2] is an integral system for performing passive containment cooling system (PCS) tests with prototypic driving forces representing the heat and mass transfer occurring within the AP600 containment. The data generated in the large-scale tests have been evaluated on several different levels. The highest level within the framework of data evaluation being performed to support the AP600 PCS performance is presented in this report. This report presents a global (rather than local) evaluation of the large-scale test data to examine the relative importance of the various parameters that affect heat removal from the vessel.

A significant amount of detailed local data evaluation has been performed to examine specific phenomena for scaling and code validation. Local data obtained from the large-scale test facility have been used to confirm the validity of the boundary layer correlations selected for modeling condensation heat and mass transfer in the AP600.[5] Evaluations of the large-scale test data have also been used to describe containment physics and quantify effects, such as sensible heating of subcooled films, evaporation, and mixing and stratification within the vessel in support of scaling studies.[3] Finally, data from the large-scale facility data are also being used to support validation of the WGOTHIC computer code.

1.0 INTRODUCTION

A design basis accident (DBA) in AP600, such as a loss-of-coolant accident (LOCA), has the potential to pressurize containment to the point of challenging the design limit of the containment shell. The AP600 passive containment cooling system (PCS) is designed to remove sufficient heat from containment during a limiting DBA to maintain peak containment pressure below the design limit and to continue to depressurize containment over the longer term. Heat is removed from the containment atmosphere by condensation and convective heat transfer to the shell. Heat is conducted through the shell and then rejected to the atmosphere on the outside of containment by convection to the buoyant cooling air, radiation to the baffle, and evaporation of the external cooling film to the cooling air.

The Westinghouse large-scale PCS test facility was built to provide test data for a geometrically similar model of the AP600 containment vessel and PCS. The tests provide experimental data that can be used for evaluating the physics in containment, determining the relative importance of various parameters that affect heat and mass transfer and validating computer codes. Three series of tests[1,2] were run at the Westinghouse large-scale PCS test facility. The steady-state pressure, annulus air flow rate, water coverage, steam flow rate, injection velocity, location and orientation, and noncondensible gas concentration were varied between the tests, as summarized in Table 1-1.

The purpose of this report is to present a global evaluation of the large-scale test data and perform comparisons to determine the relative importance of the various externally controlled parameters in affecting the heat and mass transfer. More detailed, local test data evaluations have been performed in support of the scaling analysis report,[3] the heat and mass transfer validation report[5] and the WGOTHIC code description and validation report, which is being written.

1.1 Large-Scale Test Facility Description

The large-scale PCS test facility uses a 20-ft. tall, 15-ft. diameter pressure vessel to simulate the AP600 containment vessel. The geometry is approximately a 1/8-scale of the AP600 containment vessel. A plexiglas cylinder is installed around the vessel to form the air cooling annulus. Air flows upward through the annulus via natural convection to cool the vessel, resulting in condensation of the steam inside the vessel. A fan is located at the top of the annular shell to provide the capability of inducing higher air velocities than can be achieved during purely natural convection. A liquid film can be applied outside of the test vessel to provide additional, evaporative cooling.

Test conditions (pressure, steam flow rate, cooling air flow rate, water coverage, etc.) were selected to provide heat and mass transfer validation over a range of conditions representative of a DBA.

For most of the tests, steam was injected through a diffuser located under a simulated steam generator (SG) compartment below the operating deck, as shown in Figure 1-1. The steam rises upward as a plume. Air is entrained in the rising plume, resulting in a natural circulation flow pattern and partial

mixing within the vessel. Variations in steam injection velocity and location were made to evaluate the effects on mixing and heat transfer as shown in Figure 1-2.

Approximately 300 thermocouples are installed in the test facility. Thermocouples are embedded in both the inner and outer surfaces of the vessel at various angles at 10 different elevations, as shown in Figure 1-3, to determine the temperature and flux distribution over the height and circumference of the vessel. Thermocouples are also placed inside the vessel on a movable rake to measure the bulk temperature at various locations.

The steam inlet pressure, temperature and flow; the vessel pressure; and condensate temperature and flow are measured to provide an accurate measurement of the total heat supplied to the vessel. The cooling air temperature and plexiglas surface temperature are measured at several locations in the annulus to determine the amount of convective and radioactive heat removal. The external liquid film flow rate and temperature are measured at the inlet and exit to determine the amount of heat removed by evaporation and sensible heating of the liquid film.

A more detailed description of the large-scale PCS test facility and instrumentation locations is given in Reference 2.

TABLE 1-1
LARGE-SCALE PCS TEST MATRIX

Test Number	Pressure (psig)	Flow (lb_m/sec.)	Configuration	Air Flow (ft./sec.)	Water Coverage (% Area)	Long-Term Heat Sinks	Helium	Sampling
Baseline Tests without Internals								
201.1	10	-	C3D	9	100	NO	NO	NO
202.1	30	-	C3D	9	100	NO	NO	NO
203.1	40	-	C3D	9	100	NO	NO	NO
207.1	30	-	C3D	9	75-Quad	NO	NO	NO
207.2	30	-	C3D	9	75	NO	NO	NO
Baseline Tests with Internals								
201.2	10	-	DSG - NSG	12	100	NO	NO	NO
202.2	30	-	DSG - NSG	12	100	NO	NO	NO
203.2	40	-	DSG - NSG	12	100	NO	NO	NO
204.1	30	-	DSG - NSG	16	100	NO	NO	NO
205.1	30	-	DSG - NSG	8	100	NO	NO	NO
206.1	30	-	DSG - NSG	FREE	100	NO	NO	NO
207.3	30	-	DSG - NSG	12	75-Quad	NO	NO	NO
208.1	30	-	DSG - NSG	12	50-Quad	NO	NO	NO
207.4	30	-	DSG - NSG	12	75	NO	NO	NO
210.1	40	-	DSG - NSG	12	100-Heated	NO	NO	NO
211.1	40	-	DSG - NSG	FREE	100-Heated	NO	NO	NO

TABLE 1-1
LARGE-SCALE PCS TEST MATRIX (Cont.)

Test Number	Pressure (psig)	Flow (lb_m/sec.)	Configuration	Air Flow (ft./sec.)	Water Coverage (% Area)	Long-Term Heat Sinks	Helium	Sampling
Phase 2 Tests								
202.3	30	-	DSG	12	100	NO	NO	NO
203.3	40	-	DSG	12	100	NO	NO	NO
212.1A	-	0.25	DSG	12	75	NO	NO	YES
212.1B	-	0.50	DSG	12	75	NO	NO	YES
212.1C	-	0.75	DSG	12	75	NO	NO	YES
213.1A	-	0.25	DSG	12	25	NO	NO	NO
213.1B	-	0.50	DSG	12	25	NO	NO	NO
213.1C	-	0.75	DSG	12	25	NO	NO	NO
214.1A	-	1	DSG	FREE	75	NO	NO	NO
214.1B	-	1	DSG	12	75	NO	NO	NO
215.1A	-	1	DSG	FREE	75	NO	NO	NO
215.1B	-	1	DSG	12	75	NO	NO	NO
216.1A	-	0.50	DSG	12	75-Quad	NO	NO	NO
216.1B	-	0.50	DSG	12	25-Quad	NO	NO	NO
217.1A	-	1	DSG	12	75	NO	NO	YES
217.1B	-	1	DSG	12	75	NO	[ ]^{a,b}	YES
218.1A	-	1	DSG	12	75	YES	NO	YES
218.1B	-	1	DSG	12	75	YES	[ ]^{a,b}	YES

TABLE 1-1
LARGE-SCALE PCS TEST MATRIX (Cont.)

Test Number	Pressure (psig)	Flow (lbm/sec.)	Configuration	Air Flow (ft./sec.)	Water Coverage (% Area)	Long-Term Heat Sinks	Helium	Sampling
219.1A	-	0.20	DSG	12	DRY	YES	NO	YES
219.1B	-	0.20	DSG	12	DRY	YES	[ ]^{a,b}	YES
219.1C	-	0.20	DSG	12	50	YES	[ ]^{a,b}	YES
220.1	-	Blowdown	DSG	12	75	YES	NO	YES
221.1A	-	Blowdown	DSG	12	50	YES	[ ]^{a,b}	YES
221.1B	-	Blowdown	DSG	12	DRY	YES	[ ]^{a,b}	YES
Phase 3 Tests								
222.1	-	Blowdown	DSG	12	75	YES	NO	YES
222.2A	-	Blowdown	ADD	12	75	YES	NO	YES
222.2B	30	-	ADD	12	75	YES	NO	YES
222.3A	-	Blowdown	AD3S	12	75	YES	NO	YES
222.3B	30	-	AD3S	12	75	YES	NO	YES
222.4A	-	Blowdown	AD3U	12	75	YES	NO	YES
222.4B	30	-	AD3U	12	75	YES	NO	YES
223.1	-	1.5	DSG - Vac.	12	75	YES	NO	YES
224.1	-	0.25	DSG - 2 atm.	12	100	YES	NO	YES
224.2	-	0.50	DSG - 2 atm.	12	100	YES	NO	YES

C3D - Center of vessel, 3-in. pipe at deck elevation
DSG - Diffuser in SG compartment
NSG - No steam generator model
ADD - 6-ft. above deck, diffuser
AD3S - 6-ft. above deck, 3-in. pipe, pointed sideways
AD3U - 6-ft. above deck, 3-in. pipe, pointed upward

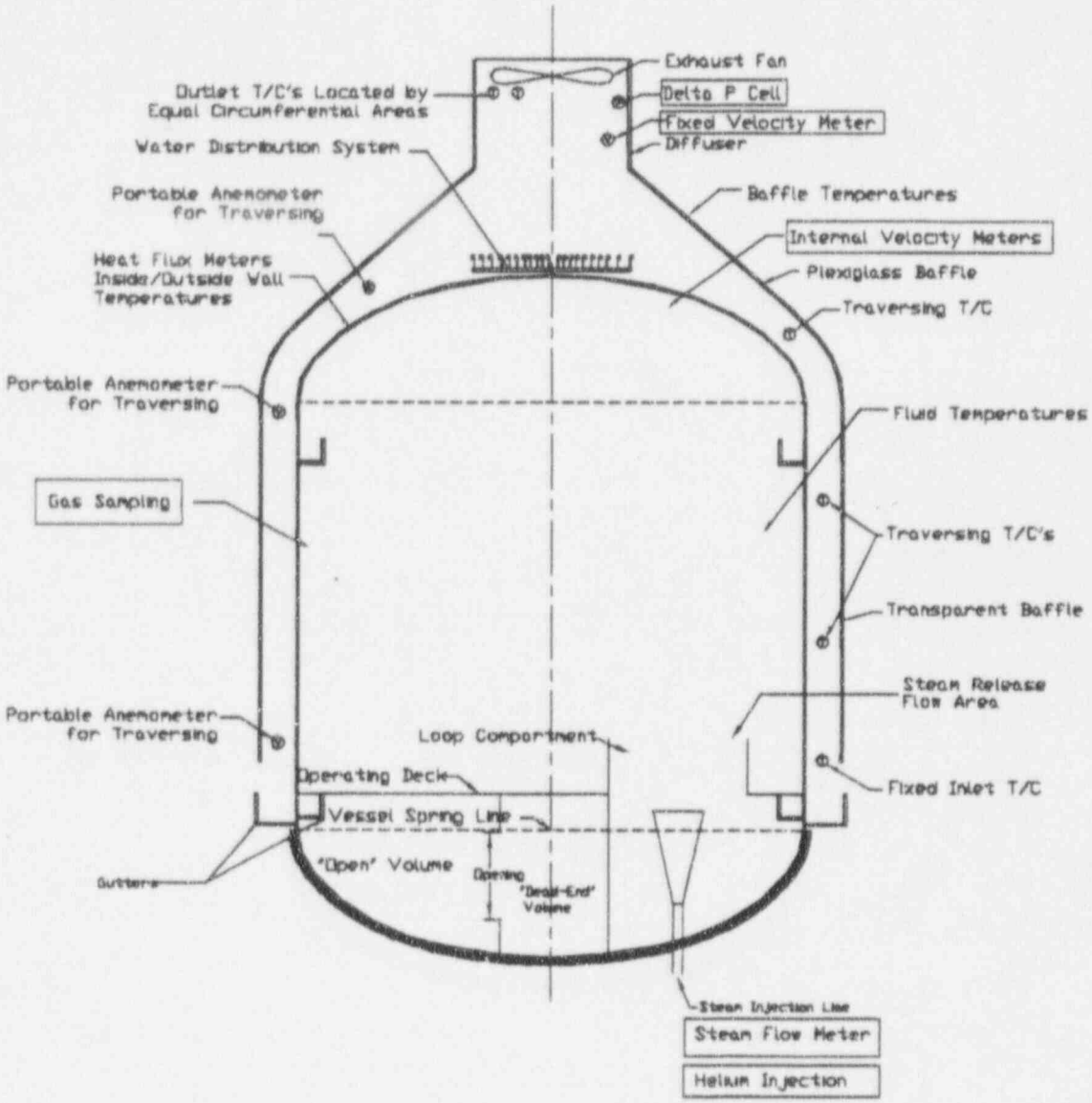

Figure 1-1 AP600 Large-Scale PCS Test Internals

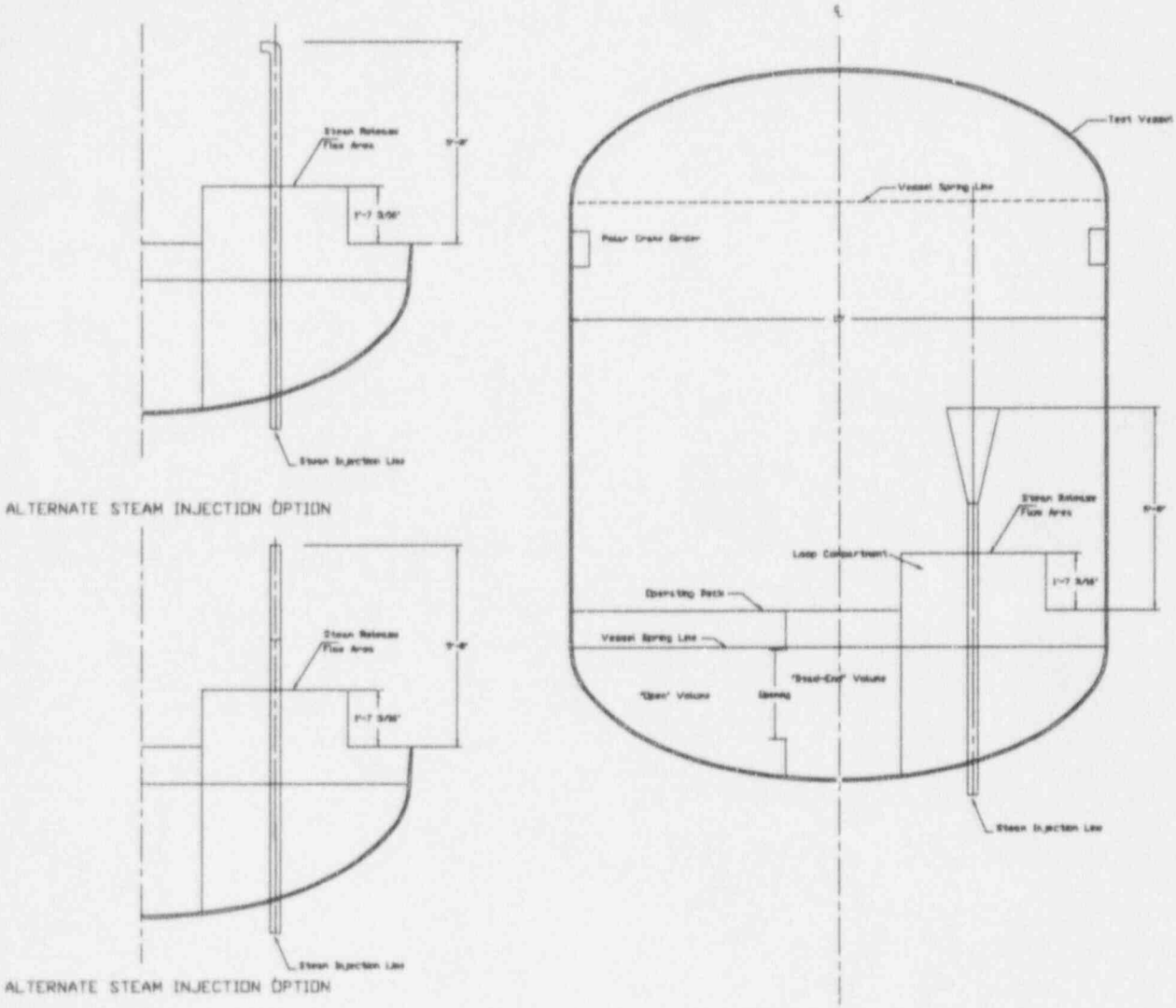

Figure 1-2 Alternate Steam Injection Locations

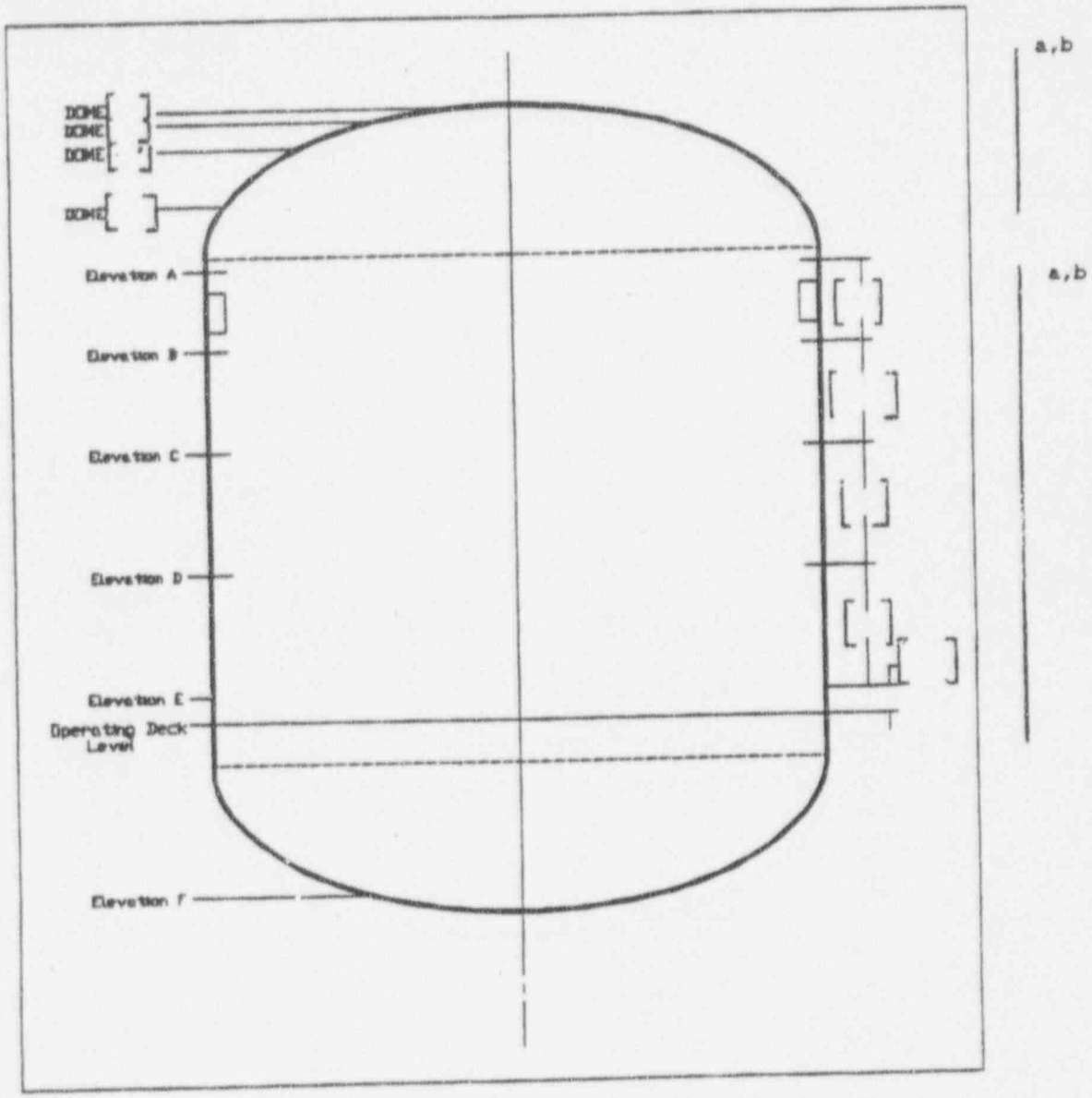

19

Figure 1-3 Large-Scale PCS Instrumentation Elevations

2.0 PARAMETRIC EVALUATION

The large-scale PCS tests provide experimental data which can be used for determining the relative importance of the various parameters that affect heat removal from the AP600. Steam is injected into the test vessel (with various velocities and at various locations) while a thin evaporating liquid film (with various flow rates and coverage areas) is applied to the outside of the vessel. Air travels upward (with various velocities and temperatures) through the annulus located between the vessel and a surrounding plexiglas cylinder. The internal vessel pressure and temperature increase until the heat addition and removal rates come into balance.

Energy is transferred between the steam/air mixture within the vessel and the inside surface of the vessel wall by convection, condensation, and conduction through the thin liquid condensate film. Qualitatively, heat removal will: increase as the temperature difference between the bulk vapor and the wall increases, increase as the steam partial pressure difference between the bulk vapor and film surface increases, and increase as the near-wall vapor velocity increases. The principal parameters that have analytically been shown to affect energy transfer to the inside of the vessel are the steam concentration and velocity near the wall;[3] conduction through the thin condensing film has been shown to be a minor resistance to heat transfer.[4] The distribution of steam inside the vessel is dependent on the degree of mixing between the steam and air. The degree of mixing is dependent on the steam source velocity (jet or buoyant plume) and injection location within the vessel. Therefore, measurements of the steam concentration distribution and internal velocity from the large-scale tests will be important in evaluating the internal heat and mass transfer.

Energy is transferred between the outside surface of the vessel and the ultimate heat sink by conduction, sensible heat addition to and evaporation from the applied liquid film, convection to the cooling air, and radiation. Qualitatively, heat removal will: increase as the temperature difference between the bulk vapor and the film on the wall increases, increase as the film coverage increases, and increase as the annulus velocity increases. The principal parameters that have analytically been shown to affect energy transfer from the outside of the vessel are: cooling air velocity and temperature, applied liquid film flow rate and temperature, and film coverage area.[3]

Assuming global quantities can be used to assess first-order effects on vessel heat transfer, the change in total vessel heat removal from one test to another can be expressed analytically using a Taylor series expansion. Using only controllable test parameters in the Taylor series expansion, the relation is:

$$\Delta \dot{Q} = \Delta C \frac{\partial \dot{Q}}{\partial C}\Big|_P + \Delta V_i \frac{\partial \dot{Q}}{\partial V_i}\Big|_P + \Delta W \frac{\partial \dot{Q}}{\partial W}\Big|_P + \Delta A \frac{\partial \dot{Q}}{\partial A}\Big|_P + \Delta T_f \frac{\partial \dot{Q}}{\partial T_f}\Big|_P + \Delta T_a \frac{\partial \dot{Q}}{\partial T_a}\Big|_P + \Delta V_o \frac{\partial \dot{Q}}{\partial V_o}\Big|_P \quad (2\text{-}1)$$

where:

- C = steam concentration distribution inside the vessel
- V_i = vapor velocity along the walls inside the vessel
- W = film flow rate
- A = film coverage area
- T_f = initial film temperature
- T_a = ambient air temperature
- V_o = annulus air velocity
- Q = total vessel heat removal rate

The overall heat removal from the large-scale test vessel is directly related to the overall heat transfer coefficient, which is a combination of the resistances on the inside and outside of the vessel. The resistance on the inside of the vessel may be larger or smaller than the resistance on the outside of the vessel. The relative importance of each parameter listed above is affected by its relation to the larger resistance. For example, a change in the internal velocity has a smaller effect on the total heat removal if the resistance to heat transfer is greater on the outside of the vessel.

Large-scale PCS test data were evaluated to determine the relative importance of each of the seven parameters in affecting the overall heat removal from the vessel. Ideally, only one of the seven parameters in Equation 2-1 would be varied, while others were held constant during the test. This would provide a value for the corresponding partial derivative term and illustrate the relative importance of each parameter. Unfortunately, this was not possible since the ambient air temperature and humidity could not be controlled, and the film temperature was controlled in only two tests. However, tests for this evaluation were selected for comparison in which the principal parameter was varied while changes in the other parameters were minimized.

The results of this global data evaluation are presented in the following subsections.

2.1 Film Flow Rate and Coverage

Based on the results of the analytical evaluation,[3] the external film flow rate and coverage area are expected to affect the heat removal rate from the outside of the vessel significantly. An increase in film flow rate (or reduction in film temperature) would increase the sensible heat removal rate and also have a second-order effect on the evaporation rate. An increase in the film coverage area would increase the total heat removal by evaporation.

The external film flow was supplied at a temperature less than its evaporating temperature and with a flow rate that was greater than required for evaporation in the large-scale PCS tests. Therefore, some fraction of the injected steam energy was removed by sensible heating of the subcooled film. The test data were evaluated to determine the fraction of the total injected energy removed by sensible heating of the subcooled film and the fraction removed by evaporation. The results from selected tests indicate that the majority of the energy (between 60 and 85 percent) is removed by evaporation. The

fraction of energy removed by sensible heating of the liquid film is between 3 and 28 percent and is higher for tests that have a lower heat flux and a higher film flow rate. The remainder is removed by a combination of convective and radioactive heat transfer.

The external water coverage for the large-scale tests was modified by either plugging the distribution J-tubes to establish a dry quadrant on the vessel, or by reducing the film flow to produce a striped water coverage (with dry stripes) on the vessel. A brief description of the striped water coverage observations is given in subsection 2.1.1. The effect on heat transfer of the two different types of water coverage is described in subsection 2.1.2.

2.1.1 Description of Film Coverage

The purpose of this section is to document observations of some of the unique aspects of wetting on the large-scale test vessel. Although wetted coverage at the bottom of the baffle was observed and recorded for all steady-state tests, documentation of the flow pattern over the dome was not part of the test specification and was only observed and noted for two tests: 222.2B and 222.4A. It was observed that the width of the wet/dry stripes was independent of the circumferential position around the vessel, but did vary from top to bottom of the vessel.

Water is applied to the dome of the large-scale test vessel by 64 small tubes connected to a common header. The tubes have an inside diameter of 0.188 in. Eight of the tubes are equally spaced (every 45 degrees) on an 11-in. diameter circle with the tube exit located 0.12 in. above the surface. The other 56 tubes are approximately equally spaced on a 61.5-in. diameter, with the tube exit located 0.5 in. above the dome surface.

Water from the inner ring of the tubes flowed in a radial pattern and flooded the surface from the 11-in. source diameter inward to the outside of the 4-in. neck flange welded to the top center of the vessel and flooded radially outward several inches beyond the source where the dry patch initiated. The width of the wet portion remained approximately constant as the water flowed outward to the second ring of tubes.

The water from the outer ring of 56 tubes formed a radial flow pattern directly below the tube, with part of the fluid flowing uphill for 2 to 3 in. The liquid film covered the entire circumference at the source and for some radial distance beyond that where (generally) stable dry patches appeared. The dry patch appeared in line with the tube, i.e., on a vessel radius that passed through the tube.

Tests 222.2B and 222.4A were observed and exhibited somewhat different wetting behavior below the steam source. The steam exited from a diffuser located 5.8 ft. above the operating deck in test 222.2B. This configuration resulted in the most extreme stratification between the upper and lower portions of the vessel of any of the large-scale tests. Steam exited from a 3-in. diameter pipe located 5.8 ft. above the operating deck in test 222.4A. This configuration produced a high-velocity

source that vigorously mixed the entire vessel, resulting in little concentration difference from the top to bottom of the vessel.

For test 222.2B, dry patches were initiated 4 to 6 in. from the source tube. There were only two or three sources that did not have an in-line dry patch, and there were no dry patches other than those inline with a source. The width of the wet stripe increased out to the drip line, where the wetted coverage was approximately 70 percent of the circumference. The wet stripes increased in width from 4 in. at the point of stable dry patching to 7.1 in. at the drip line. The wet stripes remained constant in width from the upper drip line to approximately 4 ft. above the gutter (the gutter is at the same elevation as the internal operating deck). From the 4-ft. point to the gutter, the dry portion decreased uniformly by approximately half, and many of the dry stripes disappeared completely over the bottom 8 in. of the wet surface.

The heat flux measured at the bottom of the vertical wall was approximately 1/10 that at the top of the vertical wall. The reduced heat flux below the steam source is believed to be responsible for the increase in the wetted coverage at the bottom of the vertical surface. Although the wetted surface area increased below the steam source, the wavy laminar flow pattern on the upper portion of the vertical surface continued at approximately the same width all the way to the gutter. The wetted portion that grew was visibly wet, but was not washed by waves.

The wet/dry coverage above the steam source was very stable, with little perceptible change over time. The width of the wet portion varied less than a 1/4 in. over time, but exhibited pulses in width as the thicker waves passed every few seconds. The exception was one dry streak that appeared and disappeared (over a time period of minutes). The intermittent dry patch initiated at approximately 40 degrees down the dome from the vertical centerline. In the low heat flux region below the steam source, the wet/dry interfaces showed more variability, but always greater wetted coverage than above.

For test 222.4A, dry patches began to form 6 to 18 in. from the source tube. The dry stripes were observed to widen approximately uniformly to the spring line, where the wetted coverage was 85 to 90 percent of the circumference. The wet stripes then widened uniformly, by a small amount, to the gutter. The dry streaks were more intermittent than in test 222.2B, and all dry/wet interfaces were observed to vary slowly.

2.1.2 Film Flow Rate and Coverage Effect on Heat Transfer

The quadrant and striped water coverage tests will be examined separately in this section, since they may affect the local heat transfer differently.

Baseline tests 202.2, 207.3, and 208.1 were compared to examine the effects of reducing the external water film flow rate and coverage by quadrants. A comparison of the test parameters is provided in Table 2-1. For these baseline tests, pressure was maintained at approximately 30 psig by injecting steam through a diffuser located in a simulated SG compartment below the operating deck. The

injected steam flow rate had to be decreased to maintain pressure as the film flow rate and coverage were reduced.

a,b

TABLE 2-1
QUADRANT FILM COVERAGE COMPARISON FOR BASELINE TESTS

The ratio of the film flow rates between these three tests was about the same as the ratio of the film coverages. Assuming the small differences in film temperature, air velocity, vessel pressure, and air temperature between tests did not significantly affect the comparison: an 18-percent reduction in coverage area (16-percent reduction in flow rate) resulted in a 13-percent reduction in heat rate, a 32-percent reduction in coverage area (33-percent reduction in flow rate) resulted in a 24-percent reduction in heat rate, and a 45-percent reduction in coverage area (43-percent reduction in flow rate) resulted in a 34-percent reduction in heat rate.

Heat removal from the dry portion of the vessel is primarily by convection and radiation. This is relatively small in comparison to the heat removal from the wet portion of the vessel, which is primarily by evaporation. Therefore, the energy required to maintain pressure is reduced as the fraction of the vessel area cooled by evaporation is reduced. Based on this comparison, the change in the heat removal rate is proportional to about 75 percent of the change in quadrant coverage area.

Phase 2 tests 216.1A and 216.1B were also compared to examine the effects of reducing the external water film flow rate and coverage by quadrants. A comparison of the test parameters is provided in Table 2-2. For both of these tests, steam flow was maintained at 0.6 lb_m/sec., i.e., a constant heat rate was applied while the film flow rate and coverage were reduced. The steady-state pressure increased as the film flow rate and coverage were reduced.

a,b

TABLE 2-2
QUADRANT FILM COVERAGE FOR PHASE 2 TESTS

The ratio of the film flow rates between these two tests was less than the ratio of the film coverages, i.e., the film flow rate per unit coverage area is higher in test 216.1B. However, these tests do provide some information on the pressure sensitivity to film coverage at a constant heat rate. A 68-percent reduction in the quadrant coverage area (56-percent reduction in film flow rate) resulted in a 58-percent increase in absolute pressure.

Baseline tests 207.1, 207.2, 207.3, and 207.4 were compared to examine the difference in heat removal between quadrant and striped water coverage. A comparison of test parameters is provided in Table 2-3. The pressure was maintained at about 30 psig for these tests.

a,b

TABLE 2-3
COMPARISON OF QUADRANT VERSUS STRIPED COVERAGE FOR BASELINE TESTS

Due to the differences in the inlet air velocity, tests L-207.1 and L-207.2 were compared with one another and tests 207.3 and 207.4 were compared with one another. Even though the film flow rate was smaller, the coverage area was larger in the striped coverage tests (207.2 and 207.4) and, as expected based on the quadrant coverage test comparison presented in Table 2-1, a higher heat rate was required to maintain pressure with the larger coverage area.

The increase in heat rate with coverage area (a 12-percent increase in heat rate for a 3-percent increase in area) between tests 207.1 and 207.2 was larger than expected based on the corresponding change in heat rate with coverage area that was observed in the quadrant coverage tests. The film and air temperatures decreased between tests 207.1 and 207.2, which could account for some of the increase in heat rate. Although these parameters did not seem to have much impact on the quadrant coverage tests, it was postulated that they may have an impact in the striped coverage cases. This is examined further in Section 2.2.

The increase in heat rate with coverage area (a 20-percent increase in heat rate for a 13-percent increase in area) between tests 207.3 and 207.4 was also larger than expected based on the corresponding change in heat rate with coverage area that was observed in the quadrant coverage tests. The film and air temperatures increased between tests 207.3 and 207.4. This would be expected to decrease the heat rate. This suggests that the external heat transfer also depends on the type of water coverage (striped versus quadrant). Based on this comparison, striped coverage, as would normally be expected on the AP600 vessel, provides a better surface for evaporative heat transfer than quadrant coverage. It is postulated that the striped coverage area allows for better conduction of energy from the dry stripes to the wet stripes and results in a higher average overall heat transfer coefficient from the vessel.

Baseline tests 202.1, 202.2, 207.2, and 207.4 were compared to examine the effects of reducing the external film flow rate to produce striped coverage. A comparison of the test parameters is provided in Table 2-4. The steam flow rate was adjusted to maintain pressure at about 30 psig while the film flow rate and coverage area were changed between tests. The air and film temperatures, which were not controlled, also varied between tests.

a,b

TABLE 2-4
COMPARISON OF BASELINE TESTS WITH STRIPED COVERAGE

Due to the differences in the inlet air velocity, tests 202.2 and 207.4 were compared with one another and tests 202.1 and 207.2 were compared with one another. The heat rate required to maintain a given pressure increases as the film and air temperatures decrease. For test 207.4, the film temperature was higher (which would tend to reduce the required heat rate), the air temperature was lower (which would tend to increase the required heat rate), and the film coverage area was smaller (which would tend to decrease the required heat rate). Overall, the heat rate required to maintain pressure was slightly higher in test 207.4, even though the coverage area was smaller. The higher heat rate with lower coverage area was not expected based on the results of the quadrant-coverage case comparisons. For test 207.2, the film and air temperatures were lower (which would tend to increase the required heat rate) and the film coverage area was smaller (which would reduce the required heat rate). Overall, the heat rate required to maintain pressure was lower in test 207.2 (with the lower coverage area), but the decrease was less than expected based on the results of the quadrant-coverage case comparisons. These striped-coverage comparisons indicate that the changes in the film and air temperatures also have a significant effect on the heat rate.

Phase 2 tests 202.3, 214.1B, 212.1C, and 213.1C were also compared to examine the effects of reducing the external film flow rate to produce striped coverage. A comparison of the test parameters is provided in Table 2-5.

a,b

TABLE 2-5
COMPARISON OF PHASE 2 TESTS WITH STRIPED COVERAGE

Due to the differences in the steady-state pressure, tests 202.3 and 214.1B were compared with one another and tests 212.1C and 213.1C were compared with one another. The decrease in film flow rate between tests was greater than the decrease in coverage area. The air temperature also varied between tests, but the difference in film temperature between tests was small.

The significant reduction in film coverage area and flow rate between tests 212.1C and 213.1C resulted in only a small decrease in heat rate. This was not expected based on the results of the quadrant-coverage case comparisons. The 3.5-psi increase in pressure results in an average 8°F increase in the vessel internal temperature. This, combined with the lower ambient air temperature, would tend to increase the required heat rate and offset the expected decrease in heat rate due to the reduction in film coverage. Therefore, it is believed that the increase in pressure in test 213.1C compensated for the decrease in film coverage.

The heat rate decreased as the film flow rate and coverage area decreased in test 214.1B. An 8-percent reduction in coverage resulted in a 5-percent decrease in the heat rate. This is similar to what was observed in the quadrant coverage case comparisons.

The bottom of the vessel is insulated in the phase 2 tests but not in the baseline tests, so a quantitative comparison of the results from the baseline tests with internals with the phase 2 tests is reasonable if the heat loss through the bottom of the vessel is small relative to the total heat removal. For the baseline tests with internals, the temperature difference through the vessel wall below the operating deck is much smaller (about 20 times smaller) than the local wall temperature differences above the operating deck. This indicates that the heat flux below deck is much smaller than the heat flux above

the operating deck. Therefore, since the heat flux is much smaller and the vessel surface area below the operating deck is about 28 percent of the total area, the heat loss through the bottom of the vessel in the baseline tests is small relative to the total.

As shown in Tables 2-4 and 2-5, the increase in film flow rate between baseline test 202.2 and phase 2 test 202.3 is about the same as the increase in coverage area. The difference in the film and air temperatures between these tests is not large (8°F and 13°F, respectively), so a qualitative comparison of test results between these two tests is not unreasonable. A 7-percent decrease in striped water coverage for test 202.2 (without the insulated bottom) resulted in an 8-percent decrease in heat removal.

Even though the increase in film flow rate and coverage area between baseline test 207.4 and phase 2 test 214.1B is about the same, the difference in the air temperature between these tests (33°F) is significant; therefore, a reasonable comparison cannot be made between these two tests due to the competing effects of reduced air temperature (which tends to increase the heat rate) and reduced film coverage (which tends to decrease the heat rate).

As mentioned earlier, in all of the large-scale PCS tests, the external liquid film was applied at a temperature less than its evaporating temperature and with a flow rate that was greater than required for evaporation. Although sensible heating of the subcooled film accounts for about 20 percent of the total, evaporation accounts for the majority of heat removal from the outside surface of the vessel. The heat removed by evaporation was proportionally reduced as the coverage area was forcibly reduced in quadrant-coverage cases. However, the coverage area was not controlled in the striped-coverage tests, and the heat removal rate does not appear to be as sensitive to the coverage area.

2.2 Film and Air Temperatures

As observed in Section 2.1, the striped-coverage tests seem to be more sensitive to changes in the film and air temperature than the quadrant-coverage tests and less sensitive to the coverage area. The sensitivity to the film and air temperature will be evaluated in this section.

Baseline tests 203.2 and 210.1 provide a sensitivity to the initial film temperature. A comparison of the test parameters is provided in Table 2-6.

a,b

TABLE 2-6
FILM TEMPERATURE SENSITIVITY FOR BASELINE TESTS

Even though the film flow rate was slightly lower and coverage area was slightly higher, the heat removal was slightly lower at the higher film temperature, as expected. An 18°F increase in film temperature and 12°F increase in air temperature resulted in a 4-percent decrease in heat rate. Since both the film and air temperature increased between tests, the change in the required heat rate cannot be attributed directly to the change in film temperature.

In fact, based on striped-coverage test comparisons presented in Section 2.1, the change in air temperature may have been the main contributor to the change in heat rate. As shown in Table 2-4, the heat rate increased with a small increase in film temperature and decrease in film coverage between baseline tests 202.2 and 207.4. This is opposite to the expected trend, and the increase in the required heat rate can only be attributed to the decrease in air temperature between the tests.

If a small change in film coverage (<10 percent) is assumed to be insignificant in the striped-coverage cases, then the comparison presented in Table 2-5 between tests 202.3 and 214.1B provides a good sensitivity to the air temperature. A 13°F increase in air temperature resulted in a 5-percent decrease in heat rate. This is similar to the sensitivity shown in Table 2-6 (with a smaller change in film coverage and an 18°F increase in film temperature). Therefore, a change in the air temperature appears to be more significant than a change in the film temperature in affecting the heat rate for the striped coverage tests.

2.3 Annulus Air Velocity

Baseline tests 202.2, 204.1, 205.1, and 206.1 examined the effect of changing the cooling air velocity. A comparison of the test parameters is provided in Table 2-7. The test pressure was maintained at approximately 30 psig by injecting steam through a diffuser located in a simulated SG compartment below the operating deck. The injected steam flow rate had to be increased to maintain pressure between tests as the cooling air velocity was increased.

a,b

TABLE 2-7
COOLING AIR VELOCITY SENSITIVITY FOR BASELINE TESTS

The higher cooling air velocity caused the convective heat transfer coefficient in the annulus to be higher. This affected overall heat and mass transfer, but only slightly. Comparing test 202.2 with test 206.1 (the differences in the pressure, film coverage, and air temperature between these two tests are fairly small), a 53-percent decrease in the cooling air velocity resulted in only a 7-percent decrease in the overall heat rate. This relatively weak dependence on the velocity indicates that the resistance to heat transfer on the inside of the vessel is greater than on the outside.

2.4 Steam Injection Location and Flow Rate

Condensation is the primary mode of heat removal on the inside of the vessel. Condensation mass transfer is primarily influenced by the partial pressure difference between the vapor and condensate film surface on the wall. The distribution of steam along the vessel walls, and therefore the heat removal rate, is dependent on the degree of mixing within the vessel.

The steam injection location and velocity were varied to examine how they affect mixing within the vessel. Steam was injected through a 3-in., Schedule 40 pipe located at the center of the vessel at the elevation of the simulated operating deck in the first five baseline tests. Steam was injected through a diffuser located under the SG compartment for the last 11 baseline tests and all of the phase 2 tests (see Figure 1-1). The steam injection location and velocity were varied for the phase 3 tests (see Figure 1-2).

The vessel internals were not installed for the first five baseline tests. Entrainment and natural circulation mixing of the air/steam mixture within the vessel is less restricted without the internals. Even though they are not representative of the AP600 containment geometry, these five baseline tests are acceptable for characterizing the heat and mass transfer phenomena. The internals (without the SG model) were installed for all of the remaining baseline tests; the SG model was added for the phase 2 and phase 3 tests.

The first three baseline tests (201.1, 202.1 and 203.1) were compared to examine how mixing was affected by injection velocity. The vessel was pressurized by injecting steam through a 3-in., Schedule 40 pipe located at the center of the vessel at the elevation of the simulated operating deck. For each test, a cooling air velocity of 9 ft./sec. and liquid film flow rate of about 3.19 lb_m/sec. were maintained during the steady-state test data acquisition period.

The difference in temperature between the operating deck and the top of the vessel was about 20°F at the lowest steam injection velocity (10 psig), 15°F at the intermediate steam injection velocity (30 psig), and 10°F at the highest steam injection velocity (40 psig). The axial vessel steam concentration was not measured in these baseline tests; however, it is believed that the axial temperature measurement provides some indication of the extent of the steam/air mixing within the vessel. The internal mixing, as demonstrated by the smaller axial temperature gradient, was better at the higher steam injection velocities (pressures).

Baseline tests 201.2, 202.2, and 203.2 were also compared to examine how mixing was affected by the injection velocity. These tests differ from the first three baseline tests as follows: the vessel internals were installed, the cooling air velocity was higher, and steam was injected through a diffuser located under a simulated SG compartment below the operating deck. The diffuser reduces the kinetic energy of the steam source and consequently results in a lower velocity of the steam injection plume above the operating deck.

The difference in temperature between the injection location and the top of the vessel was about 10-12°F in all three tests; however, the temperature just above the bottom of the operating deck, elevation E, was significantly lower than the temperature just above the injection location, elevation D (see Figure 1-3 for locations). The difference in temperature above and below the injection location (23°F at 10 psig, 19°F at 30 psig and 12°F at 40 psig) was dependent on the injection velocity, decreasing as the velocity (pressure) was increased. Although a measurement of the internal fluid temperature below the operating deck was not available, the inner vessel wall temperatures below the operating deck were lower in these tests than tests 201.1, 202.1, and 203.1. Based on these larger axial temperature gradients in the vessel, the internal mixing of vapor above with vapor below the injection elevation was significantly reduced after the diffuser and lower internals were installed. This was verified by the noncondensible gas measurements in later tests.

Since a main steam line break in the AP600 plant could occur either above or below the operating deck, phase 3 tests 222.2B, 222.3B, and 222.4B were compared to examine how changing injection velocity and direction affected the mixing above the operating deck. For these three tests, the injection location was placed 5.8 ft. above the operating deck. The steam was injected through a diffuser in test 222.2B and through a 3-in. diameter pipe in tests 222.3B and 222.4B. The injection angle was changed from horizontal to upward between tests 222.3B and 222.4B.

As determined from temperature measurements being nearly constant with elevation above elevation C, the steam and air within the vessel are well mixed above the injection point in test 222.2B. There is a

40°F temperature drop between elevations C and D and another 80°F temperature drop between elevations D and E . The temperature at elevation F was not measured; however, the wall temperature was about 50°F lower than the temperature at elevation E. Therefore, injection through the diffuser located above the deck caused a large temperature stratification below the injection location, indicating that there is very little mixing below the injection location. This was verified by the noncondensible gas measurements.

The high velocity jet from the 3-in. diameter pipe caused the entire vessel to be well mixed in both tests 222.3B and 222.4B. The upward direction of the injection angle in test 222.4B caused temperatures at the top of the dome to be slightly higher; however, the measured temperature below the operating deck was within 7°F of the temperatures above deck.

Inner wall temperatures are lower at the top of the dome than along the cylindrical sidewalls (above the injection location) in all of the tests except 222.3B (high velocity, horizontal steam injection). Since vapor temperature and steam concentration are both higher at the top of the dome, condensation heat and mass transfer (and consequently the heat flux) is expected to be higher at the top of the dome. Indeed, for all of the tests except 222.3B, the highest heat flux (based on measured wall temperature differences) occurred where the external liquid film was applied near the top of the dome. The average heat flux is shown as a function of the heated length (distance along the inner wall surface from the operating deck elevation to the top of the dome) for a typical phase 2 test (212.1A) in Figure 2-1. For test L-222.3B, the highest heat flux occurred on the wall opposite the jet, just above the jet elevation, as shown in Figure 2-2.

Even though the heat flux is higher near the top of the dome, heat transfer from the walls may be a more significant fraction of the total since heat transfer area per unit length increases with distance from the top of the dome and reaches a maximum on the cylindrical wall. Total heat removal from the dome was compared with total heat removal from the cylindrical walls for a typical phase 2 test, 212.1, and the well-mixed phase 3 test, 222.4B. Approximately 40 percent of the heat was removed from the dome and 60 percent was removed from the sidewalls in both tests. Note that the dome is about 30 percent of the heat transfer area. Therefore, the ratio of heat removal from the dome and sidewalls was not affected by the better vessel mixing in test 222.4B; and even though the heat flux was higher near the top of the dome, the total heat removal from the cylindrical sidewalls was higher than the dome.

The heat removal rate for test 222.2P (most stratified with a diffuser located 5.8 ft. above the deck) was compared with test 222.4B (well mixed with high-velocity jet from a 3-in. pipe located 5.8 ft. above the deck) to examine the effect of mixing. The results are presented in Table 2-8.

a,b

TABLE 2-8
MIXING SENSITIVITY FOR PHASE 3 TESTS

The heat rate required to maintain the vessel pressure at 45 psia is about 35 percent higher in the stratified test. The higher injection velocity (and corresponding higher velocity along the walls) in test 222.4B may also affect the comparison; however, heat removal in a stratified vessel appears to be better than in a well-mixed vessel.

2.5 Effect of Helium Injection

A high concentration of noncondensible gas near the condensing surface would inhibit mass transfer. Noncondensible gas concentrations were measured near the top of the dome and at the bottom of the vessel during some of the phase 2 and phase 3 tests. These measurements indicated that air was concentrated in the volume below deck in all but the high-velocity steam injection phase 3 tests.

The injection of a light noncondensible gas (helium) will cause the pressure to increase and possibly alter condensation heat and mass transfer to the inside surface of the vessel. Phase 3 tests 217.1, 218.1, and 219.1 examined the effect of helium injection on heat transfer. For the first two tests, the vessel was allowed to reach steady state with a constant steam and liquid film flow rate prior to the helium injection. The vessel was kept dry in test 219.1 until after the helium injection was complete. Helium was released at a constant rate over a 30-minute period. Gas concentrations were measured at four different locations within the vessel every hour over the next several hours until the vessel reached a well-mixed, steady-state condition.

The helium concentration was well mixed above the operating deck throughout the test, but there was initially little helium below the operating deck. As the test continued, helium began to mix below the deck as well, and about 2 hours after the injection, the entire vessel was well mixed.

In test 219.1C, the external water film was applied about 3 hours after the helium injection was complete. The helium concentration did not stratify, but continued to be well mixed throughout the vessel.

A comparison of the test results is presented in Table 2-9.

a,b

TABLE 2-9
HELIUM GAS SENSITIVITY FOR PHASE 2 TESTS

The injection of helium increases the vessel pressure as expected based on the volume of gas injected, but it appears to have little impact on the heat removal rate.

[ ]a,c

Figure 2-1 Heat Flux versus Heated Length for Test 212.1A

a,c

Figure 2-2 Heat Flux versus Heated Length for Test 222.3B

3.0 CONCLUSIONS

The evaluation of large-scale PCS test data yielded the following information and conclusions:

- Evaporation was the primary mode of heat removal from the outside of the vessel (approximately 75 percent of the total), followed by sensible heating of the subcooled liquid film (approximately 17 percent of the total). The remainder of the heat was transferred to the environment by convection and radiation.

- The heat removal rate was proportional to the film coverage area in quadrant-coverage cases, but had a weak dependence on the coverage area in striped-coverage cases. For the same film coverage area, striped coverage provided better heat removal than quadrant coverage.

- The heat removal rate appeared to be more strongly dependent on ambient air temperature than liquid film temperature.

- The heat removal rate has a relatively weak dependence on annulus air velocity, which indicates that the resistance to heat transfer on the inside of the vessel is greater than on the outside.

- For all of the wetted large-scale tests (except the horizontal, high-velocity steam jet injection case), the highest heat flux occurred near the top of the dome at the elevation where the external film was applied. Although the dome represents about 30 percent of the heat transfer surface area, approximately 40 percent of the total heat removal occurred on the dome and 60 percent on the cylindrical sidewalls.

- Injection of low-velocity steam resulted in relatively good mixing above the injection location, but stratification below, causing air to be concentrated below the operating deck. The heat removal rate increased as the axial steam concentration gradient was increased (by raising the injection location).

- Injection of high-velocity steam resulted in a well-mixed vessel (both above and below the operating deck).

- Injection of a light, noncondensible gas did not degrade the condensation heat transfer or affect the overall heat removal. The gas did not stratify (collect at the top of the vessel), but was well mixed above the injection location and eventually, well mixed throughout the entire vessel.

4.0 REFERENCES

1. Peters, F. E., *AP600 1/8th Large Scale Passive Containment Cooling System Heat Transfer Test Baseline Data Report*, Rev. 1, WCAP-13566, October 1992.

2. Peters, F. E., *Final Data Report for PCS Large-Scale Tests Phase 2 and Phase 3*, WCAP-14135, July 1994.

3. Spencer, D., *Scaling Analysis for AP600 Passive Containment Cooling System*, WCAP-14190, October 1994.

4. Spencer, D., Westinghouse AP600 Letter Report, *Liquid Film Model Validation*, January 1994, Docket No.: STN-S2-003.

5. Ofstun, R. P., *Experimental Basis for the AP600 Containment Vessel Heat and Mass Transfer Correlations*, WCAP-14326, March 1995.